

Lithographically Fabricated 10-Micron Scale Autonomous Motors

Yang Wang¹, Shih-to Fei¹, Vincent H. Crespi², Ayusman Sen,¹ and Thomas E. Mallouk^{1*}

¹Department of Chemistry, Pennsylvania State University, University Park, PA, 16802, U.S.A.

²Department of Physics, Pennsylvania State University, University Park, PA, 16802, U.S.A

ABSTRACT

Self-propulsion and directed movement of nano- and micro-particles can in principle provide novel components for applications in microrobotics and MEMS. Our research involves the design of catalytic propulsion systems and the control of colloidal movement based on this principle. We have designed autonomous nanomotors that mimic biological motors by using catalytic reactions to generate forces derived from chemical gradients. Through architectural control of bimetallic catalytic particles, we have recently developed systems that undergo more complex movement. For example, we have constructed 10-micron scale rotary motors by contact lithography. In these chiral motors, bimetallic Au-Pt patterns are free-standing and move in the pattern predicted by theory. These studies demonstrate that by designing the proper architecture, one can tailor the pattern of movement to specific applications, such as changing from translational to rotational movement. The potential for elaboration of these designs to more complex micro-machine assemblies is discussed.

INTRODUCTION

We describe the lithographic fabrication of catalytic propulsion systems in various new designs that control/tailor movement patterns from translational to rotational at the 10 μ m scale. Nano- and sub-microscale autonomous moving systems have attracted substantial interest because of potential applications in powered assembly, delivery vehicles, MEMS, robotics, fluidics, and sensing. Nano- and microscale movement driven by catalysis is an expanding area that follows from the recent discovery of autonomous nanomotors that mimic biological motors by using catalytic reactions to generate forces derived from chemical gradients^{1,2}. Template-grown bimetallic nanorods can move at speeds up to 30 μ m/s by catalyzing the decomposition of hydrogen peroxide. An electrokinetic mechanism for powered movement has been proposed for these systems^{3,4}, and several subsequent studies have expanded on the idea to demonstrate enzymatically catalyzed and rapid directional movement^{5,6}. A significant restriction in nanomotor research is that they generally rod-shaped, although some interesting efforts have been made to modify the nanorod geometry^{7,8} to achieve more complex movement such as rotation. The template growth of nanorods thus significantly limits the possible applications for this system. One way to address this problem is to use contact lithography, which provides the freedom to design and fabricate microscale objects that have arbitrary planar geometries.

One concern in designing new nano- and micromotor shapes is the issue of scaling. Catalytic nanomotors work in the low Reynolds number regime, and at larger length scales, inertial propulsion mechanisms can become dominant. Catchmark et al have demonstrated lithographically fabricated 150 μ m diameter microgears that rotate in hydrogen peroxide with an activation pretreatment that changes the hydrophobicity of the metal surface⁹. At larger length scales, Ismagilov and Whitesides observed catalytic movement driven by bubble recoil.¹⁰ Based on simple scaling arguments as well as these empirical observations, one can anticipate changes

in the propulsion mechanism over length scales of tens to hundreds of μm . To investigate this question and gain insight to the parameters that are important in catalytic motor design, we have studied the fabrication of 10 μm scale motors based on Au-Pt lithographic patterning. We designed a rotary motor in order to study its behavior as a function of geometrical parameters and to confirm the dominant role of electrokinetically driven movement at this length scale.

EXPERIMENTAL SECTION

Conventional contact microlithography was used to build the motor structure. The design was based on a two layer alignment process. A 100 nm Cu metal layer was evaporated onto 3-inch Si wafers as the sacrificial layer. Two photomasks were designed on LEDIT and then written on a Heidelberg Laser writer on a soda lime 4 inch mask. The masks were used in conventional photolithography to transfer patterns onto photoresist/lift-off resist (Shipley SPR1805 and LOR2A). LOR2A was first spun onto the Cu coated 3-inch Si wafer at 2000 rpm for 60s, baked at 180°C for 6min, followed by a coating of photoresist 1805 at 4000 rpm for 40s, soft-baked at 115°C for 1min, and then exposed through the aligned mask for 1.5 s using a mercury-lamp ultraviolet source calibrated to an exposure output of 12mW/cm² on a Karl Suss MA-6 optical contact aligner. The exposed photoresist was developed in 0.26 N tetramethylammonium hydroxide for 1 minute. Pt and Au metals were evaporated onto the patterned surface and then lifted off by submerging the wafer into acetone for 10 h, followed by rinsing in isopropanol and DI water. The liftoff resist (LOR) was stripped by submerging the wafer into tetramethylammonium hydroxide for 30min and then in DI water. The motors were released from the wafer into solution by remove the Cu sacrificial layer in 30% ammonia solution for 1 hour. The solution was centrifuged 5 times and replaced with DI water. The catalytic movement of the resulting structures was tested by mixing with H₂O₂ solution and observed under microscope. The motion was tracked through PhysVis free software developed by Kenyon College.

RESULTS and DISCUSSION

Design and fabrication of the rotor

A rotary motor, shown in Figure 1, was fabricated lithographically, with the Pt strips patterned onto a rectangular piece of Au. The idea behind this design is that a motor arranged in a chiral fashion will spin. Fig. 1 shows a C₂-symmetry design that should generate a net torque around the center of mass and promote rotation. A long Pt bar with a “leading edge” outside the Au area was included in the design in an attempt to direct the driving force in the plane of the rotor rather than in the vertical direction.

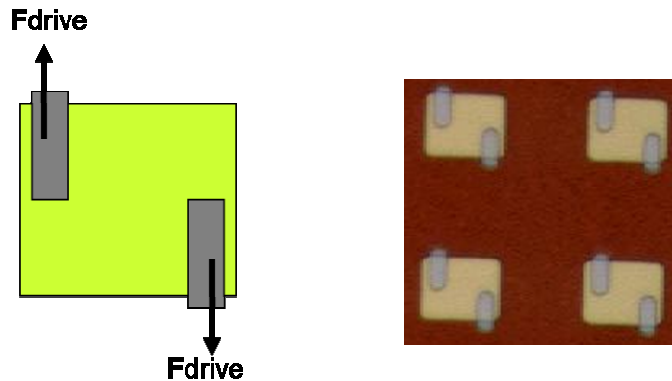


Figure 1: Left: the scheme and force analysis of an $8\mu\text{m} \times 10\mu\text{m}$ Au square with chiral Pt corner elements; Right: the optical image of the lithographically fabricated Pt-Au micro-objects when they are still on the wafer.

The actual sum of the generated torque will determine the rotation direction, which should be greatly influenced by the dominant mechanism in such a system: If it is electrokinetic mechanism, they should rotate clockwise with Pt end forward (as shown in figure); if bubble recoil dominates, the rotors should rotate counter-clockwise as the force of the recoil will cause the gold end to move forward. In the case of the surface tension driven model,⁹ the rotor should not move since our experimental procedure does not promote the hydrophobicity of either metal.

Movement of the rotor in aqueous hydrogen peroxide

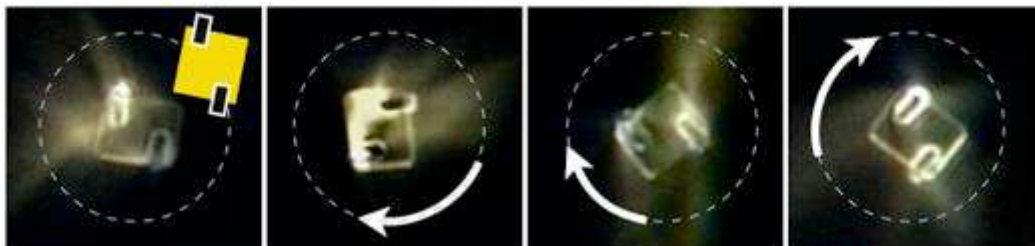


Figure 2: An $8\mu\text{m} \times 10\mu\text{m}$ Au square with chiral Pt corner elements rotates at 0.5 rad/s in $15\% \text{H}_2\text{O}_2$

In aqueous hydrogen peroxide, the lithographically fabricated motors rotate with a speed of 10~15 rpm, with the Pt features as the leading end (clockwise). 80% of the motors spin clockwise; and less than 20% of them spin counter-clockwise. The observed direction of movement is consistent with a dominant bipolar electrochemical mechanism on this length scale. In addition, the nucleation of gas bubbles was not observed on the motors themselves but rather on the surrounding glass surfaces, further suggesting that the mechanism of energy transduction was not the same as in the macroscopic recoil driven systems. At the same time, the rotors showed no evidence of surface tension driven motion, especially considering the surface wetting condition of the rotors – If a significant amount of surface area is sufficiently hydrophobic, the surface tension of the water should be able to destabilize the rotors or even cause the light rotors

to float. Instead, the rotors remained stable at the bottom of the solution. All these phenomena support a bipolar electrochemical mechanism.

The rotational speed is lower than what would be expected from our experience with the nanorod system, which is may be due to several factors: First, the design did not result in a fully horizontal motor assembly, so some of the force generated will still be directed in the vertical direction and will not contribute to rotational movement. Second, the contact area with the floor of the container is relatively large compared to the functional Pt component, so the effect of surface friction would also be large compared to a rod system. The surface quality and thus the catalytic activity of metal patterned through lithography may also be a concern. Finally, as the length scale increases the edge area of the catalytic surface increases linearly, and the mass of the motor increases as the square of the length (assuming constant thickness). Numerical modeling of the catalytic reaction and forces as a function of scale will be needed to understand the relative contributions of these factors.

CONCLUSIONS

Rotors fabricated by lithographic methods are fully functional at the 10 μ m scale, and their observed direction of movement supports the electrokinetic mechanism as the dominant driving force. It should be possible to further increase the speed of the rotors, and by utilizing the flexibility of lithographic fabrication we should be able to induce more complex movement, or perhaps even promote cooperative behavior such as two-dimensional self-assembly.

ACKNOWLEDGMENTS

Financial support for this project was provided by the Penn State Center for Nanoscale Science (NSF-MRSEC under grant DMR-0820404).

REFERENCES

1. W. F. Paxton, K.C. Kistler, C.C. Olmeda, A. Sen, S.K. St. Angelo, Y. Cao, T.E. Mallouk, P.E. Lammert, V.H. Crespi, *J. Am. Chem. Soc.* 126, 13424 (2004)
2. S. Fournier-Bidoz, A.C. Arsenault, I. Manners, and G.A. Ozin, *ChemComm.* 441 (2005).
3. Y. Wang, R. Hernandez, D. Bartlett, J. Bingham, T. Kline, A. Sen, T. E. Mallouk, *Langmuir*, 22, 10451 (2006)
4. W. F. Paxton, P.T. Baker, T.R. Kline, Y. Wang, T. E. Mallouk, and A. Sen, *J. Am. Chem. Soc.* 128, 14881 (2006)
5. N. Mano, A. J. Heller, *J. Am. Chem. Soc.* 127, 11574 (2005)
6. R. Laocharoensuk, J. Burdick and J. Wang, *ACS Nano* 2 (5), 1069 (2008)
7. Y. He, J. Wu, and Y. Zhao, *Nano. Lett.* 7 (5), 1369 (2007)
8. L. Qin, M.J. Banholzer, X. Xu, I. Huang, C.A. Mirkin, *J. Am. Chem. Soc.* 129 (48), 14870 (2007)
9. J.M. Catchmark, S. Subramanian, and A. Sen, *Small*, 1(2), 202 (2005)
10. R. F. Ismagilov, A. Schwartz, N. Bowden, G.M. Whitesides, *Angew. Chem. Int. Ed.* 41, 652

(2002)